

Review of *Ventilation and low pollution enhancing new particle formation in Milan, Italy*

Agrò et al.

An error in Figures S9 (title) and S10 (x-axis label) was identified in the previous version of the responses to the referees' comments and has been corrected in this revised version. In addition, the sentence describing SO₂ behavior (Fig. S9b) has been revised. Minor editorial changes were also made, including small wording revisions, a clarification regarding the sulfuric acid proxy time series, and the addition of a missing reference.

The authors thank the referees for their effort in reading and providing positive and constructive feedback for the improvement of this article. Below, we report in red the referees' comments and in black the authors' answers. In the authors' reply, *italic purple* is used to report text from the previous version of the manuscript, while *italic blue* is used for the updated text.

During the review of the article, the authors found an error in the background subtraction step of the nano-particle ranking method. The error has been corrected, and Fig. 6, 7, 8, 9, 10, 11, 12, 14, S3, S4, S5, S6 (now S4, S5, S6, S7) have been updated. Overall, the figures remain similar to the previous version, and the conclusions of the study remain unchanged.

At line 156, the percentage of data availability was changed from days to time for clarity.

Finally, Federico Bianchi was added as corresponding author at Line 20. In addition, minor changes to the references were made, as well as minor grammatical and stylistic revisions.

Answer to Anonymous Referee #2

This manuscript presents a unique and innovative year-long dataset of particle number size distributions (1.2–480 nm) collected in the urban background of Milan using advanced instrumentation. Through statistical analysis of these data combined with meteorological and pollution conditions, the authors show that new particle formation (NPF) events are favoured under relatively clean atmospheric conditions—with lower pollutant concentrations, reduced condensation sink, and stronger ventilation—whereas stagnant conditions within the Po Valley inhibit NPF. The study is highly relevant and I recommend it for publication in ACP after considering the following comments.

We thank Anonymous Referee #2 for this positive comment.

Major comments

* My main concern is that the manuscript combines data from very different atmospheric conditions (e.g., varying levels of pollution, ventilation, and meteorological regimes)

without sufficiently distinguishing between them in the analysis. By aggregating these diverse situations, the results risk being biased or leading to misleading conclusions, as the mechanisms controlling NPF occurrence and growth are strongly dependent on background conditions. For example, clean-air episodes driven by strong northwesterly winds are fundamentally different from stagnant periods within the Po Valley in terms of condensation sink, precursor availability, and atmospheric dynamics, but are these conditions more frequent in winter than summer when NPF is expected to be more frequent? I strongly recommend that the authors stratify their dataset according to representative regimes (e.g., different seasonal contexts or maybe clean vs. polluted and ventilated vs. stagnant,) and assess NPF occurrence separately. This would not only reduce potential biases but also strengthen the scientific insights and policy relevance of the study. Additionally, a more explicit discussion of the limitations and uncertainties associated with mixing these conditions would help clarify the robustness of the conclusions.

We thank both referees for highlighting the potential bias introduced by combining different atmospheric regimes. We acknowledge their doubts regarding the stratification of the dataset and the possible biases arising from treating different atmospheric conditions together. The limited amount of data does not allow for a deep stratification. However, to assess the referees' concerns, a comparison of the NPF relevant variables during stagnant ($VI < 400 \text{ m}^2\text{s}^{-1}$) and non-stagnant ($VI > 400 \text{ m}^2\text{s}^{-1}$) periods and in different seasons was performed.

The following discussion was added as a new subsection in the article at Line 457. The numbering of the subsequent sections was adjusted as needed.

“3.5 NPF drivers in different atmospheric regimes”

The results described so far were obtained using the entire dataset regardless of the environmental conditions. However, treating different atmospheric regimes, such as ventilated and stagnant conditions or different seasons together may create biases in the interpretation of the drivers of NPF and hide potentially relevant patterns.

To evaluate the robustness of our conclusions in different regimes, we performed an additional stratified analysis separating stagnant and non-stagnant conditions and different seasons (see Supplementary Materials) and applying the nano-particle ranking analysis on each subset. The two analyses (seasons and stagnant/non-stagnant) were performed separately, and the stratifications were not combined due to the limited amount of data.

Despite the differences in background conditions, the main conclusions did not change when analyzing separately stagnant and non-stagnant periods. CS values were generally higher under stagnant conditions compared to non-stagnant ones; however, in both regimes, the CS decreased with increasing NPF rank, indicating that stronger NPF

preferentially occurred under lower CS conditions, independently of the level of stagnation (Fig. S9a). SO₂ concentrations showed a less clear behavior and did not appear to limit NPF both under stagnant and non-stagnant conditions (Fig. S9b). Sulfuric acid proxy and J₃ increased with NPF rank in both regimes (Fig. S9c, Fig. S9d).

Considering that seasonality may have still introduced some bias in the interpretation of these results (Table S1), a separate study for each season was performed.

Seasonal stratification revealed higher CS values in winter compared to the other seasons. In winter and autumn, the CS clearly decreased with increasing NPF rank, while this relation was weaker in spring and summer (Fig. S11a). J₃ was more difficult to interpret on a seasonal basis, particularly in summer, due to the limited data availability. Nevertheless, J₃ generally increased with NPF rank in all seasons, consistently with the results from the non-stratified dataset (Fig. S11e).

SO₂ concentrations were generally higher in winter than in the other seasons due to the enhanced emissions and the weaker dispersion conditions. In winter, SO₂ showed a decreasing trend with increasing NPF rank (Fig. S11c), in agreement with the opposite relation between NPF rank and SO₂ observed in the non-stratified analysis. In spring, summer, and autumn, SO₂ concentrations were lower and did not exhibit a clear trend with NPF rank. Similar SO₂ levels associated with both weak and strong NPF events suggest that SO₂ availability was not a limiting factor for NPF intensity during these seasons. The sulfuric acid proxy did not show a clear relation with NPF rank in most seasons, except for autumn, when an increasing trend was observed (Fig. S11d).

The analysis of NPF after stratifying different atmospheric conditions does not contradict the results obtained with the entire dataset. However, drawing conclusions may be misleading. In fact, the stratification led to a low amount of data per class, reducing the reliability of the results. Furthermore, the NPF intensities in the different groups (seasons, stagnant and non-stagnant) may not be comparable, considering that the nano-particle ranking was applied separately on each subset (Fig. S10). To assess this, the concentration of 2.5-5 nm particles was also used as proxy for NPF intensity other than the percentile rank (Fig. S11f, Fig. S11g).

A larger dataset would allow a more in-depth analysis of how different regimes may affect NPF and of the main drivers of this process in various atmospheric conditions.”

The plots and table regarding this analysis have been reported below and included in the following section of the Supplementary Materials:

“NPF drivers in different atmospheric regimes

To assess the characteristics of the NPF drivers in different atmospheric regimes, the dataset was first separated into stagnant and non-stagnant days using the threshold set by ARPA Lombardia of $VI=400\text{ m}^2\text{ s}^{-1}$. Then the nano-particle ranking method was applied

to each of the two subsets and the variables CS, formation rates, SO_2 concentration, and sulfuric acid proxy were analyzed in relation to NPF ranks. Finally, the full dataset was divided into seasons and the same analysis was performed.

The results obtained for the stagnant vs. non-stagnant analysis are reported in Fig. S9.

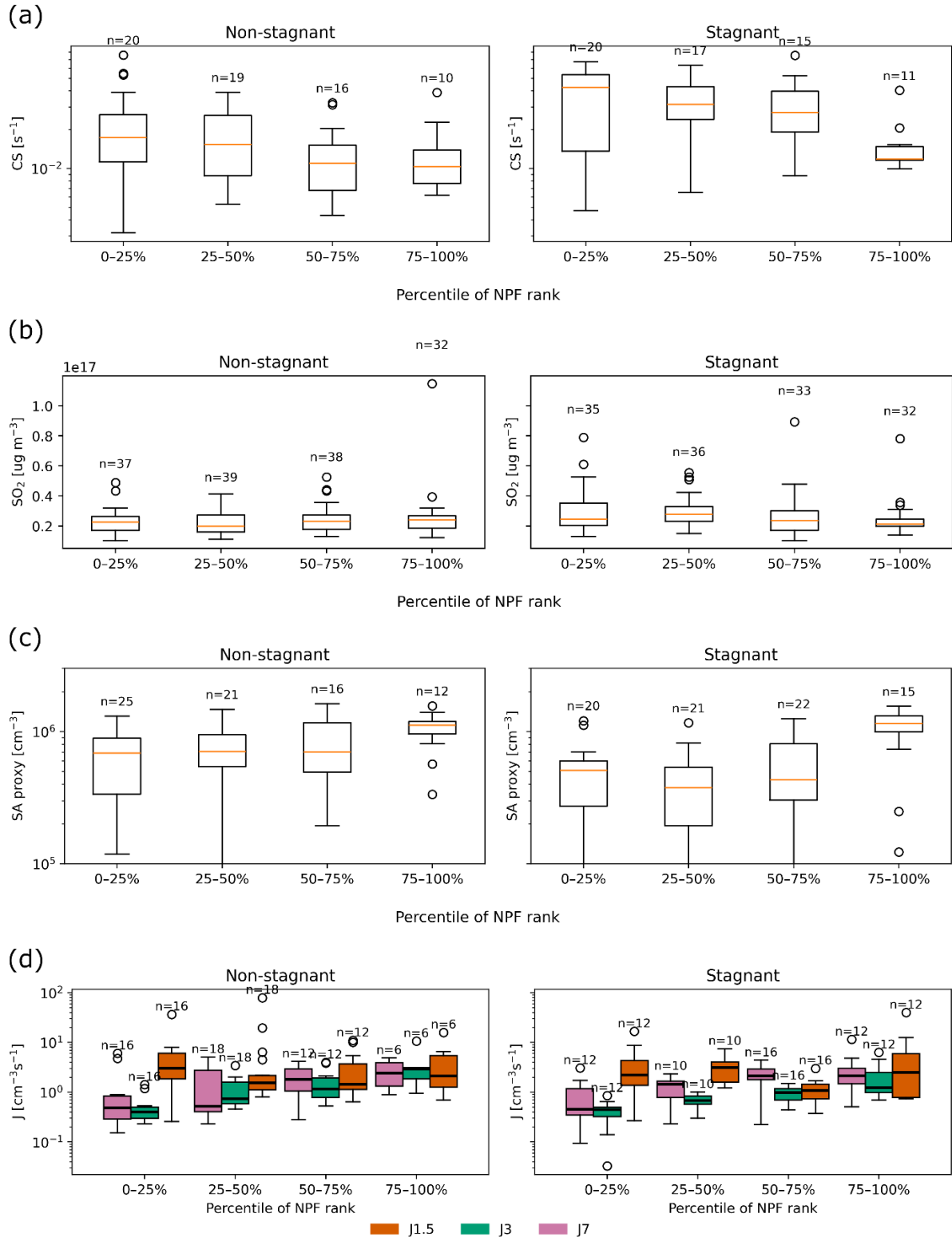


Figure S9: Daily a) median CS, b) median SO_2 , c) median SA proxy calculated over the active time window of each day per rank class during stagnant and non-stagnant conditions; d) daily maximum $J_{1.5}$, J_3 , and J_7 during the active window of each day, per rank class during stagnant and non-stagnant conditions. n indicates the number of datapoints included in the boxplot. For the description of the boxplot, see Fig. 4b.

The NPF intensities (concentration of 2.5-5 nm particles) were overall higher during non-stagnant conditions (Fig. S10):

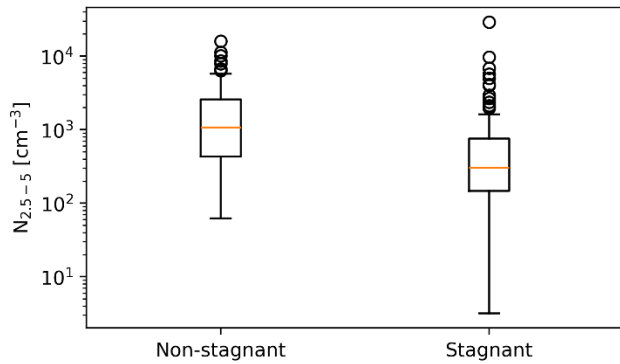


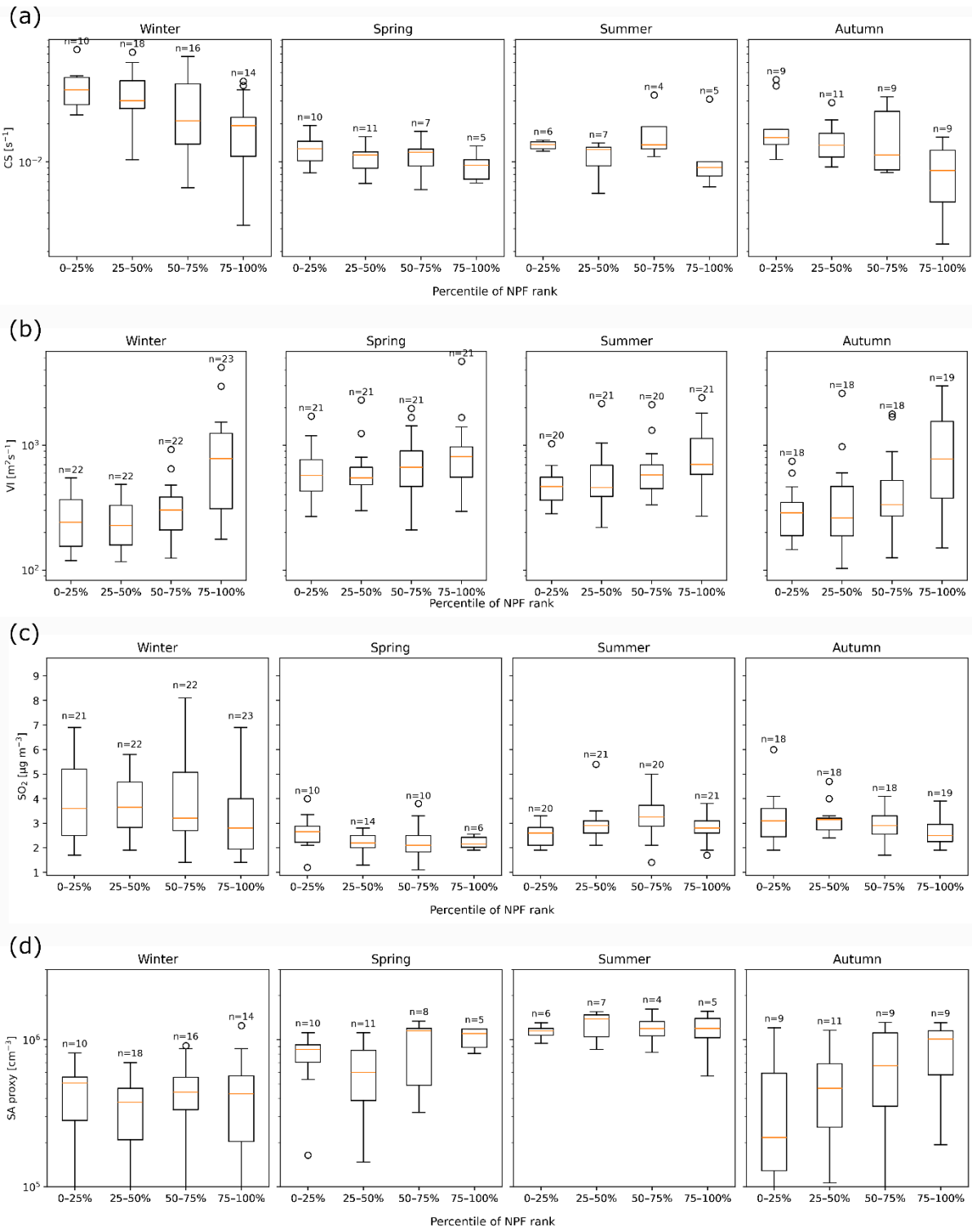
Figure S10: $N_{2.5-5}$, representing NPF intensity, as explained in Sect. 2.4.1, during stagnant and non-stagnant conditions. Boxplots are defined as in Fig. 4b.

Seasonal effects may further bias this analysis as more stagnant days were recorded during autumn and winter and non-stagnant days in summer and spring (Tab. S1):

	Stagnant	Non-stagnant
Autumn	42	31
Spring	18	66
Summer	22	60
Winter	65	24

Table S1: Number of stagnant and non-stagnant days per season.

The results from the seasonal analysis are reported in Fig. S11:



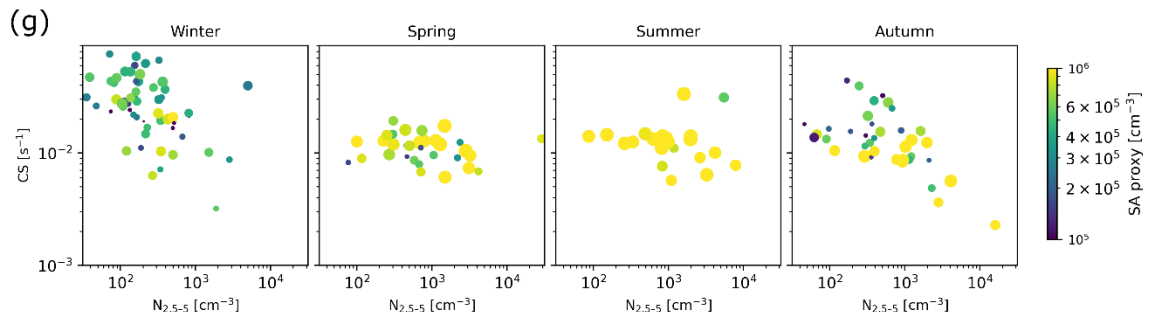
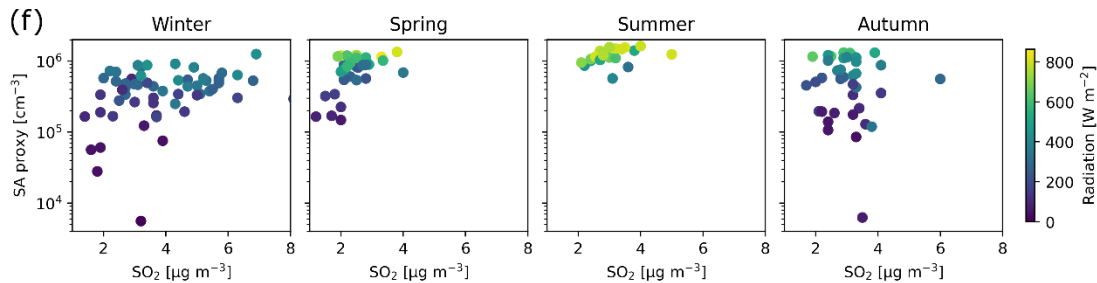
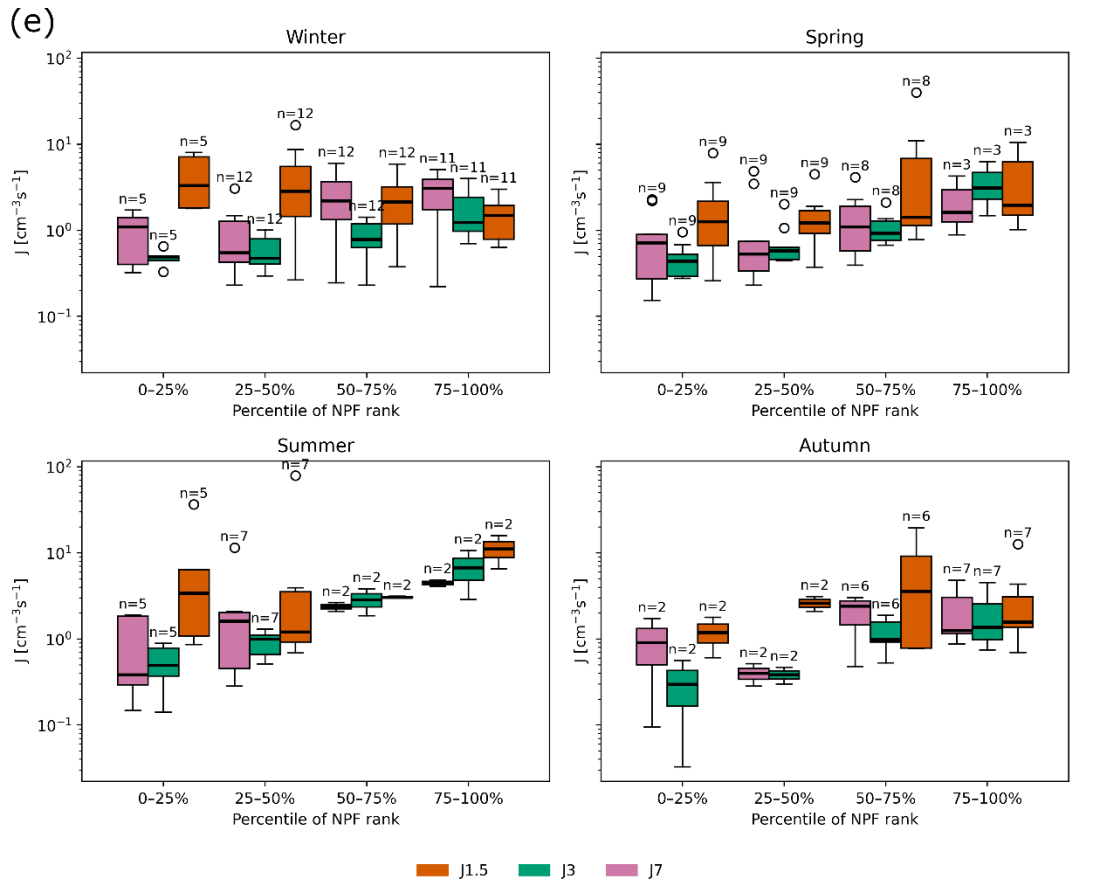


Figure S11: Daily a) median CS, c) median SO_2 , d) median SA proxy calculated over the active time window of each day, per rank class in different seasons; b) daily VI per rank class in different seasons; e) daily maximum $J_{1.5}$, J_3 , and J_7 during the active window of each day, per rank class in different seasons. n indicates the number of datapoints included in the boxplot. For the description of the boxplot, see Fig. 4b; f) relation between the daily median SA proxy, radiation, and SO_2 calculated over the active time window in different seasons; g) relation between the daily median CS, $N_{2.5-5}$, SA proxy, and radiation (size of the dots) calculated over the active time window in different seasons.”

Minor comments

Section 2.2 – The manuscript states that different PNSDs are combined, but it is not specified which size ranges from each instrument are ultimately considered after corrections. For example, does the 15 nm data come from the NAIS or the SMPS? Similarly, is the 2.2 or 3 nm range taken from the NAIS or the nCNC? Figure 3 shows the median PNSD, but was this calculated only for periods when all instruments were operating simultaneously? Finally, since the NAIS was installed in a different building, the authors should discuss whether this could introduce uncertainties. Have inlet losses been quantified and corrected?

Particle number size distributions from the nCNC and the NAIS were combined at 2.2 nm, while those from the NAIS and the SMPS were combined at 25 nm. To further clarify this, the sentence “*Then, the size distributions of the three instruments were combined at 2.2 nm and 25 nm*” (Line 165) was changed to “*Then, the number size distributions from the three instruments were combined using the concentrations measured by the nCNC for the particles smaller than 2.2 nm, by the NAIS for the particles in the 2.2-25 nm size range, and by the SMPS for the particles larger than 25 nm.*”

Figure 3 shows the median particle number size distribution calculated using only the periods when the three instruments were measuring simultaneously. The following sentence was added at Line 163: “*for the periods when all three instruments were operating simultaneously.*”

The following sentence was also added in the caption of Fig. 3: “*The medians were calculated using only the periods when all the instruments were measuring simultaneously.*”

We are aware that installing the NAIS in a separate building may have indeed introduced some uncertainties. The reason for this different location was logistical, as a big enough room was not available to host all the instruments. However, both buildings faced the university’s inner yard, representative of the urban background and lacking a specific source (for example, none of the inlets faced a road regardless of their location in different buildings). Therefore, we believe that the combination of the data from these instruments is still reasonable. To clarify this in the manuscript as well, the following sentence was added at Line 130: “*While the difference in location between the NAIS and the other instruments may have introduced some uncertainty, all inlets faced the interior of the University’s yard, which is not constantly affected by one specific source (for example, traffic), and can, therefore, be considered representative of Milan urban background. For this reason, the combination of the data by these instruments was considered reasonable regardless of their different location.*”

Finally, inlet losses were taken into account and corrected for the PSM and NAIS data (Lines 145 and 156). The SMPS TSI Aerosol Instrument Manager program was used to invert the SMPS data, and it did not account for inlet losses (Line 153).

L146-148 – what about polystyrene latex particles (PSL) calibration and in situ intercomparison with a total CPC?

The authors are not aware whether PSL calibration was performed for the SMPS before the measurements.

In situ intercomparison with a total CPC was not performed as a total CPC was not available at the site.

L176 – I recommend using the terminology “eBC – equivalent black carbon” rather than “BC – black carbon” (Savadkoohi et al., 2024).

The following change was made at Line 176: “*black carbon (BC)*” → “*equivalent black carbon (eBC, Savadkoohi et al., 2024)*”. For consistency, the change was also made at lines 384, 462, 468, 473, 489, in Fig. 15a and Fig. S5 (now Fig. S6).

L177-179 – The BLH is estimated using two different models depending on conditions, but the methods are insufficiently explained. Given that the ventilation index is a key parameter throughout the manuscript, further explanation of these methods and their limitations is required.

The following detailed explanation of the methods for the calculation of the BLH was added at Line 176.

“ARPA Lombardia also provided BLH data from the nearby station of Milano Parco Nord. The BLH was estimated using the Gryning-Batchvarova model for the daytime convective boundary layer (Batchvarova and Gryning, 1991) and the Zilitinkevich model for the nocturnal stable boundary layer (Zilitinkevich and Baklanov, 2002). Both models used turbulence variables that were measured by ARPA Lombardia with a triaxial ultrasonic anemometer at the Milano Parco Nord station. The choice of the appropriate model was based on the assessment of the boundary layer stability, determined from the sensible heat flux, also measured by the ultrasonic anemometer at the same site.

Briefly, the Gryning-Batchvarova model describes the daytime convective boundary layer using a simplified analytical approach. The profiles of the main variables are schematized considering that, throughout the boundary layer, each variable assumes a constant value equal to its vertical mean, the entrainment layer is considered to be of infinitesimal thickness, and that, at the entrainment layer, there is a characteristic discontinuity for each variable. For the assessment of the stable boundary layer, Zilitinkevich et al. (2007) developed theoretical models considering simple equilibrium regimes in a step-by-step approach. They applied Large Eddy Simulation to validate their theoretical multi-limit BLH formulation, which reduces to known asymptotic limits in the neutral and nocturnal

stable regime. Indeed, the stable and neutral BLH evolution is controlled by factors (e.g., baroclinic shear, large-scale vertical velocity at the top of the boundary layer, non-stationarity of the boundary layer and its horizontal heterogeneity) that are difficult to measure and to use for the validation of the theory.”

L195 – CET time is UTC+1 or UTC+2 depending on the period of the year?

All times are in UTC+1 regardless of the period of the year for consistency. This is specified at Line 195.

L226 – “condensation sink (CS).”

“Condensation Sink (CS)” was changed to “condensation sink (CS)”. For consistency, the following changes were made:

Line 21: *New Particle Formation (NPF)* → *New particle formation*

Line 36: *New Particle Formation (NPF)* → *New particle formation*

Line 187: *Ventilation Index (VI)* → *ventilation index (VI)*

Line 194: *Nano-particle ranking* → *nano-particle ranking*

Line 228: *Source-Receptor Relationship (SRR)* → *source-receptor relationship (SRR)*

Line 266: *Air Mass Exposure (AME)* → *air mass exposure (AME)*

Line 463: *Air Mass Exposure* → *air mass exposure*

Line 464: *Ventilation Index* → *ventilation index*

Line 499: *Source-Receptor Relationship (SRR)* → *source-receptor relationship (SRR)*

Figure 13: *Ventilation Index* → *Ventilation index*

Figure 13: *Air Mass Exposure* → *air mass exposure*

Figure 15: *Air Mass Exposure* → *Air mass exposure*

Figure 15: *Wind Speed* → *Wind speed*

Figure 15: *Relative Humidity* → *Relative humidity*

L247-251 – “growth rate (GR)”. What is meant by “the days above the 80th percentile rank,” and why is this metric used instead of the daily GR? If this choice is motivated by uncertainty in GR, how does the uncertainty compare with that introduced by selecting only the 80th percentile?

Growth Rate (GR) was changed to *growth rate (GR)* at Line 255. The GR was estimated using the daily median size distribution surface plot calculated over all days with NPF

rank above the 80th percentile. To clarify this in the manuscript, the following change was applied at Line 247:

ORIGINAL: “*Considering the limited variability of the GR values (Kulmala et al., 2022), the median size distributions of the days above the 80th percentile rank was used to calculate the average GR in the size ranges of 3–7 nm, 7–20 nm, and 20–100 nm with the maximum concentration method (Kulmala et al., 2012) to evaluate $J_{1.5}$, J_3 and J_7 respectively (Kerminen et al., 2018).*”

MODIFIED: “*Considering the limited variability of its values (Kulmala et al., 2022), the GR was estimated using the daily median size distribution surface plot calculated over all days with NPF rank above the 80th percentile. The GR was computed for the size ranges of 3–7 nm, 7–20 nm, and 20–100 nm with the maximum concentration method (Kulmala et al., 2012) to evaluate $J_{1.5}$, J_3 , and J_7 , respectively (Kerminen et al., 2018).*”

The reason why the GR was calculated on the average size distributions of the days over the 80th percentile is that only a very limited number of days over the entire dataset exhibited a clear enough growth to allow the calculation of the GR using the traditional methods, such as time of appearance or maximum concentration (Kulmala et al., 2012). While this approach, indeed, introduces some uncertainty, it was chosen in order to have a GR value to compute in the formation rate calculation for every day, regardless of how clear the growth identification was to the eye. As mentioned at Line 247, this choice is supported by the findings of the study by Kulmala et al. (2022), reporting a limited variability of the GR. Although uncertainties are introduced, the authors still preferred to assign a GR value to each day, rather than excluding the days for which the growth was not clear (most days) from the J calculation. To assess and discuss the uncertainty associated with our method, the following section was added to the Supplementary Materials:

“Discussion on the uncertainty of the growth and formation rates estimation”

To assess the uncertainty associated with our method for the estimation of the growth and formation rates, we computed the GR for those days when a clear growth pattern was visible and when all the instruments were measuring simultaneously using the maximum concentration method (Kulmala et al., 2012). The number of days with these characteristics was 9 for the calculation of GR_{3-7} and GR_{7-20} , and 7 for GR_{20-100} .

*For clarity, in this discussion, the original method described in the article, and using the average size distributions of the days with NPF rank above the 80th percentile, is defined as **method 1**. The alternative method, consisting of the day-by-day estimation of the GR, is referred to as **method 2**. The GR and J calculated with the two approaches are reported in Fig. S3. Although GR_{3-7} and GR_{7-20} calculated with method 1 do not fall within the interquartile range of those calculated with method 2 (Fig. S3a), the limited amount of data points included in the boxplot could potentially create a bias in the comparison.*

The J values obtained with the two methods remained very similar (Fig. S3b). A day-by-day comparison showed that the relative differences in the estimated J values were always below 10%, with the exception of four cases, which still remained below 21%.

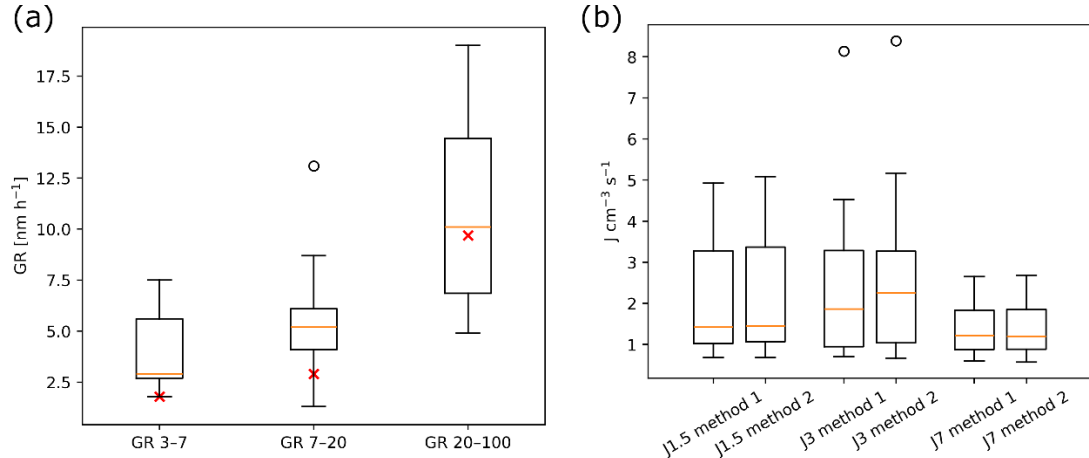


Fig S3: a) Boxplots representing the GR estimated using method 2, compared to the GR calculated using method 1 (in red x marks); b) comparison between formation rates calculated using the GR from method 1 and 2. The boxplots include only the days when the estimation of GR (and therefore J) with method 2 was possible. For the description of the boxplots, refer to Fig. 4b.”

This discussion is referenced in the article at Line 251:

“The uncertainty associated with this method for the estimation of GR and J is discussed in the Supplementary Materials.”

Section 3.1 – Is the amount of data available sufficient to be representative of each season? Does it make sense to combine the size distributions when not all three instruments were operating?

The authors believe that the amount of data available is sufficient to be representative of all seasons for most of the conclusions. While the nCNC and SMPS datasets contain several gaps, especially in summer, the NAIS, the data of which were also used to apply the nano-particle ranking method, provided a good data coverage over the entire year. Therefore, the conclusions based on Fig. 9b, 10, 11, 12, and 14a (now in Supplementary Materials) remain valid for all seasons, as no average nCNC and SMPS data were used.

We acknowledge that Fig. 8, 9a, 13, and 14b (now 14a) are affected by the limited and uneven data availability and therefore may not equally represent all seasons. To clarify the limitations of the dataset, the following sentences were changed/added:

- Line 377: “As mentioned in Sect. 2.4.4, formation rates were calculated only for the days when all the instruments were measuring simultaneously and, therefore, the data availability shown in Fig. 2 should be taken into account when interpreting Fig. 8.”

- Line 390: “As reported in Sect. 2.4.3, the CS was calculated only for the days when both the SMPS and NAIS provided good data availability. As a result, the CS time series contains several gaps (Fig. 2), which affect Fig. 9a.”

- Line 441: “Considering the data availability described in Fig. 2, the number of data points used in the calculation of the average concentrations shown in Fig. 13 may vary depending on the diameter.”

- Line 453: “The gaps in the CS time series due to the limited SMPS data coverage are reflected into the SA proxy time series and may affect Fig. 14.”

Finally, the choice of using all data despite the differences in the coverage of the instruments comes from the wish to provide a broader picture of NPF in Milan in all seasons, which we believe is possible due to the extensive data coverage of the NAIS. We acknowledge that combining average size distribution surface plots from instruments with different data availability has limitations and may be misleading. Therefore, we chose to show all the available data, still making sure that the reader was aware of the different coverages through the bar plots on the side of Fig. 4a (now 5a) and 6.

Figure 4 – Is there a physical explanation for the decrease in concentrations in the 1–3 nm size range? In addition, figures should include the minimum and maximum values of the axes.

The reason for the gap in the 2–3 nm size range is not clear. While uncertainties related to instrumental losses can not be excluded, several physical factors can play a role. In particular, different processes affect the sub-2 nm and >5 nm particles, creating different modes. Only with very intense local NPF, the gap wouldn’t be present. However, the detailed determination of the reasoning behind this gap would require a modeling approach and it is beyond the scope of this study.

The minimum and maximum values of the axes were not included for graphical reasons.

L309-314 – I recommend including particle number concentration values in Milan compared with other southern European cities. Additionally, consider including the N/BC ratio (as an indicator of the contribution of primary and secondary particles) to strengthen this section and compare with other locations.

Regarding the comparison between concentrations in Milan and in other sites, the following paragraph was added:

“Other than this qualitative comparison, a quantitative one was also performed, and the concentrations in the nucleation, Aitken, and accumulation modes measured in Milan were compared with the values reported for other European cities. The average number concentrations for particles in the 10–25, 25–100, and 100–480 nm size ranges were 2642 cm^{-3} , 4080 cm^{-3} , and 1819 cm^{-3} , respectively. Regarding the accumulation mode, Milan fell within the typical southern European cities, characterized by high concentrations of particles in this size range. The Aitken mode in Milan exhibited a lower average concentration compared to other southern European cities (4800 – 5900 cm^{-3}) but lay at the upper end of the range reported for central European cities, characterized by

intermediate concentrations in this mode. Finally, intermediate concentration values were recorded in the nucleation mode in Milan.

This comparison, though, should be interpreted with caution as it may be affected by several uncertainties. In fact, while the data presented by Trechera et al. (2023) refer to the years 2017-2019, the data presented in this study cover a single year (2023-2024), characterized by several gaps in the data availability, affecting especially the calculations in the Aitken and accumulation modes. Moreover, differences in the instruments cut-off diameters may further bias this comparison.”

The following paragraph was added to qualitatively assess the relative contribution of primary and secondary emissions in Milan compared to other European cities:

“The ratio between the average particle number concentration in the nucleation mode (N_{10-25}) and eBC was used to qualitatively assess the relative contributions of primary and secondary emissions in Milan compared to other European urban background sites. Milan exhibited an intermediate-low N_{10-25} /eBC ratio ($\sim 1444 \text{ cm}^{-3} \mu\text{g}/\text{m}^3$), within the approximate range of 900-4500 calculated for other cities (Trechera et al., 2023). This suggests that primary emissions (traffic) dominated the nucleation mode particles in Milan, whereas in other European sites, photochemistry played a more significant role.”

Finally, the following sentence was added at Line 367, in the J analysis:

“This result agrees with the discussion in Sect. 3.1 about the relevant role of traffic compared to photochemistry in Milan in the 10-25 nm size range.”

L319-322 – Please use the term “total particle number concentration” consistently, and add “number” at L322.

“Total particle concentration” was changed to “total particle number concentration”. For consistency, the following changes were also made:

- Line 54: *UFP concentrations* → *UFP number concentrations*
- Line 75: *UFP concentrations* → *UFP number concentrations*
- Line 133: *concentrations* → *number concentrations*
- Line 241: *particle concentrations* → *particle number concentrations*
- Line 301: *particle concentrations* → *particle number concentrations*
- Line 305: *particle concentrations* → *particle number concentrations*
- Line 328: *total particle concentration* → *total particle number concentration*
- Line 333-334: *particle concentration* → *particle number concentration*
- Line 335: *particle concentration* → *particle number concentration*
- Line 347: *UFP concentrations* → *UFP number concentrations*
- Line 492: *particle concentrations* → *particle number concentrations*

L315-324 – From a reviewer's perspective, this paragraph could be removed, as the discussion on whether the new air quality directive is appropriate is not sufficiently developed and does not fit within the scope of this manuscript. I think is not the place to open the question if the new air quality directive is appropriate or not.

The authors understand the referee's point and agree that further discussion on the new air quality directive is needed, but beyond the scope of this article. However, we believe this paragraph shows relevant results to support the importance of this study and of sub-10 nm particle measurements. As this perspective was probably not clear in the first draft, the paragraph was moved to Sect. 2.2 and revised as follows:

"The relevance of UFP has led the European Union to enforce the measurement of their number concentration. As reported in Sect. 1, a 10 nm cut-off was chosen to define UFP. In Fig. 4, the total particle number concentration for different cut-off sizes was calculated by integrating the size distribution from different lower limits (2 nm, 5 nm, and 10 nm) to the upper limit of 480 nm. In our dataset, lowering the threshold from 10 nm to 5 nm would result in an average increase of 14%, whereas adopting a 2 nm cut-off would lead to a 19% increase (Fig. 4a). Fig. 4b shows the variability of the ratio between the concentration for a certain cut-off size (2, 5, 10 nm) and the total particle number concentration. These considerations highlight the potential impact of measurement thresholds on reported UFP number concentrations and emphasize the importance of detailed measurements of sub-10 nm particles. While the availability and complexity of the instrumentation pose significant challenges to measuring sub-10 nm particles, the dataset presented in this work demonstrates the value of extending the measurements below 10 nm."

The numbering of Fig. 4 and 5 was adjusted as needed.

The sentence at Line 103 was changed from *"By presenting a dataset of particle number size distributions extending down to 1.2 nm, we also 104 evaluated the influence of the 10 nm cut-off diameter of the European air quality directive 2024/2881 on reported particle 105 number concentrations in urban Milan."* to *"By presenting a dataset of particle number size distributions extending down to 1.2 nm, we also show the importance of extending size distribution measurements below 10 nm, especially in relation to the European air quality directive 2024/2881."*

L355 – GR values are means or medians?

The GR values at Line 355 were calculated using the daily median size distribution surface plot for the days above the 80th percentile of NPF rank, as described in Section 2.4.4. With this method, only one GR per size range was obtained. Therefore, the reported values are neither medians nor means.

L357 to Fig. 8 – Could J_3 be lower than J_7 because of the decrease in PNSD previously mentioned for Figure 4?

It is possible that J_3 is lower than J_7 because of the decrease in concentrations around 3 nm, observed in Fig. 4 (now Fig. 5). However, a physical meaning of this can not be excluded. As mentioned in the reply to the comment above about Fig. 4 (now Fig. 5), the particles below and above 3 nm undergo different processes, producing separate modes. Only in the case of strong NPF the gap is not observed, and, indeed, in the case of NPF rank above the 80th percentile, the median of J_3 is higher than the median of J_7 . However, several different processes are involved, and assessing the characteristics of this gap in detail is beyond the scope of this work.

L375-377 – While CS is lower in summer than in winter, precursor concentrations and chemistry also vary between seasons. The conclusions drawn here are too strong given that different factors are not isolated (look major comment).

The following change was applied not to bias the reader's understanding while still describing Fig. 9.

ORIGINAL: “*Therefore, it is clear that cleaner air conditions and stronger atmospheric mixing correlated with enhanced NPF. In particular, intermediate-strong NPF (percentile rank > 60%) happened, on average, only during non-stagnant days and low CS (< 0.007 s⁻¹ on average).*”

MODIFIED: “*Therefore, enhanced NPF was, on average, associated with cleaner air conditions and stronger atmospheric mixing. In particular, intermediate-strong NPF (percentile rank > 60%) happened mostly during non-stagnant days and when the CS was relatively low (< 0.007 s⁻¹ on average).*”

Section 3.4 – The anticorrelation between SO_2 and H_2SO_4 may be influenced not only by CS but also by radiation. Likely SO_2 is higher in winter, when nano ranking is lower(?). How much do the observed H_2SO_4 concentrations contribute to the calculated growth rates?

The relation between SO_2 , SA, CS, radiation, and NPF was analyzed in more detail, and the new conclusions are reported in the answer to Anonymous Referee #3.

The contribution of sulfuric acid to the GR was calculated using Eq. 5 from the work by Nieminen et al. (2010), assuming $\rho_d = \rho_v$ and $\gamma = 1$. With this approach, we obtained that sulfuric acid contributed only to the 4%, 2% and 0.6% of GR_{3-7} , GR_{7-20} , and GR_{20-100} , respectively. These values become more uncertain at larger sizes as the approximation $\gamma = 1$ starts failing. Furthermore, the sulfuric acid concentrations used in this calculation are only a proxy and are likely lower than the actual atmospheric concentrations, considering the values measured in another Po Valley site and reported by Cai et al. (2024). The fact that the calculated GR are so low further supports that the sulfuric acid proxy underestimates the concentrations and only its trend must be interpreted, but not its values. For these reasons, the estimation of the contribution of sulfuric acid to the GR was not added to the article.

Answer to Anonymous Referee #3

The manuscript “Ventilation and low pollution enhancing new particle formation in Milan, Italy” describes the characteristics of the particle number size distribution in an urban setting. The aerosol measurements are combined with meteorological measurements and modeling to provide context for the observed variations in particle number and size. Given that the measurements are made in an urban environment, there are implications for air quality management. I think that the manuscript is acceptable for publication following consideration of my comments below.

We thank Anonymous Referee #3 for the positive feedback.

Comments:

- Overall: The manuscript provides a high-level overview of the measurements with most of the analysis centered on the percentile of NPF rank. This choice was probably made to keep the analysis and complexity at a reasonable level. However, given the seasonal variation that occurs in the physical drivers of NPF (precursor concentration, boundary layer height, potentially transport direction and/or clean vs stagnant conditions, etc.) and the fact that many of these drivers co-vary, this overview analysis potentially hides important details that would further advance “...our understanding of the state and behaviour of the atmosphere and climate” (ACP scope). I encourage the authors to consider if it would be more appropriate to consider the rank analysis after already segmenting the data based on a given condition (season, transport regime, or something similar). This would increase the scientific contribution and policy relevance of the results. In the absence of such an analysis, the manuscript must include a more comprehensive discussion about the potential biases/complicating factors of doing the analysis on the complete data set.

We understand the referee’s concern. This topic was assessed in the reply to the major comment by Anonymous Referee #2.

- Figure 2: Given the lack of data in the summer months, how robust are the conclusions for this time period? While this would be challenging to evaluate, the manuscript should discuss this limitation in greater detail and should consider if it is appropriate to “sell” this as a year of measurements or if only fall, winter, and spring should be considered.

This concern was discussed in the answer to Anonymous Referee #2.

Technical:

- Sect 2.2: Please describe the inlets (material, length, flows, etc.) that were used for the particle instruments. It would also be good to comment on the magnitude

of the correction required in different size ranges for the inlet losses. This provides the reader with important details to understand associated uncertainty.

The following sentences were added/modified in the article to better describe the inlet systems:

Line 136: “The AND inlet consisted of a 40 cm stainless steel tube sampling ambient air at a flow rate of about 6 L min^{-1} , while the PSM, connected to the AND through a conductive tube, worked with a flow rate of 2.5 L min^{-1} . The nCNC measured in scanning mode with saturator flow scanning between 0.1 L min^{-1} and 1.3 L min^{-1} .”

Line 144: “The SMPS (Wang and Flagan, 1990), consisting of a 3080 TSI classifier, a 3081 TSI DMA, and a 3772 TSI CPC, was equipped with a stainless steel inlet drawing 1 L min^{-1} of ambient air”

Line 150: “The NAIS was equipped with a 50 cm copper inlet followed by a downward bend to prevent rain from entering the instrument, resulting in a total inlet length of approximately 60 cm. Ambient air was sampled at a flow rate of 54 L min^{-1} . The instrument measured in particle, ion, and offset mode, changing mode every 90 seconds. Instrument cleaning was performed when needed.”

Inlet losses were estimated for the nCNC and the NAIS. For the NAIS, they were between about 15% at 0.8 nm and about 0.1% at 40 nm. The nCNC inlet losses ranged between 9.3 and 20%, depending on the particle size. The following sentences were changed/added:

Line 140: “The data from the nCNC were inverted using the kernel inversion method and applying the corrections for the background, the detection efficiency, the dilution factor, and the inlet losses, estimated to be between 20 and 9.3%, depending on the particle size (Lehtipalo et al., 2022).”

Line 152: “The data were then corrected for inlet losses (between 15% and 0.1%, depending on the particle size; Gormley and Kennedy, 1948) and ion calibration (Wagner et al., 2016).”

SMPS losses were not accounted for in the analysis of the SMPS data.

- Sect 2.2: Inlet cleaning is mentioned several times. Did the cleaning have any noticeable effect on the measurements? If so, is there any drift/bias associated with the measurements (due to time since cleaning)?

The cleaning procedures that were performed on the three instruments were done following the manufacturers' instructions. While cleaning can potentially affect the measurements, especially if not properly done, not performing any cleaning would create inevitable errors in the data. The NAIS, for example, records

artificially high concentrations of particles in specific size bins when the electrometers are noisy due to the deposition of dirt. Cleaning such electrometers is essential to reduce the noise and therefore prevent the recording of high concentrations that are, though, just due to instrumental issues and do not reflect ambient concentrations.

- Sect 2.4.3: Please specify if the condensation sink was calculated using dry particles or if assumptions about water were made.

No assumptions were made about water, as the authors did not have enough information about the hygroscopic parameters. The following sentence was added at Line 232:

“, using the original data without making assumptions about water. This introduces some uncertainty in the CS values as the NAIS measured a wet flow while the SMPS one was dried.”

In the same section, a mistake was found and corrected in Eq. 3:

$$\text{“}CS = 4\pi D \sum_{d_p'} \beta_{m,d_p'} d_p' N_{d_p'}\text{,”}$$

While the use of the dryer in the case of the SMPS was already stated in the article, the following sentence was added at Line 136 to highlight the role of the AND diluter as a dryer too:

“Using a dry flow for the dilution, the AND also acted as a dryer.”

It's relevant to highlight that the NAIS flow was not dried, given the inlet flow rate of 54 L min⁻¹. To specify this, the following statement was written at Line 150:

“Considering the high inlet flow rate of the NAIS, drying the sample flow was not possible.”

- Line 262: Please provide additional information on the CHIMERE model (reference, version, etc.).

The reference to CHIMERE was actually deleted as the final version of the analysis did not include results from the CHIMERE model. The sentence at Line 262 was changed from *“In this study, we modified the AME calculation by incorporating FLEXPART output with dynamic, three-dimensional emissions data from the CHIMERE model, including its temporal variations”* to *“In this study, we modified the AME calculation by incorporating FLEXPART output with three-dimensional emissions (calculated as mentioned in section 2.4.2), including temporal variations, following the approach used by Bettineschi et al. (2025).”*

- Figure 4: Please include a color bar scale. Please consider changing the number of data points to equivalent days of data (or hours). This would be easier for the reader to interpret.

The colorbar of Fig. 4 (now Fig. 5) was added and the number of data points was changed to number of equivalent days.

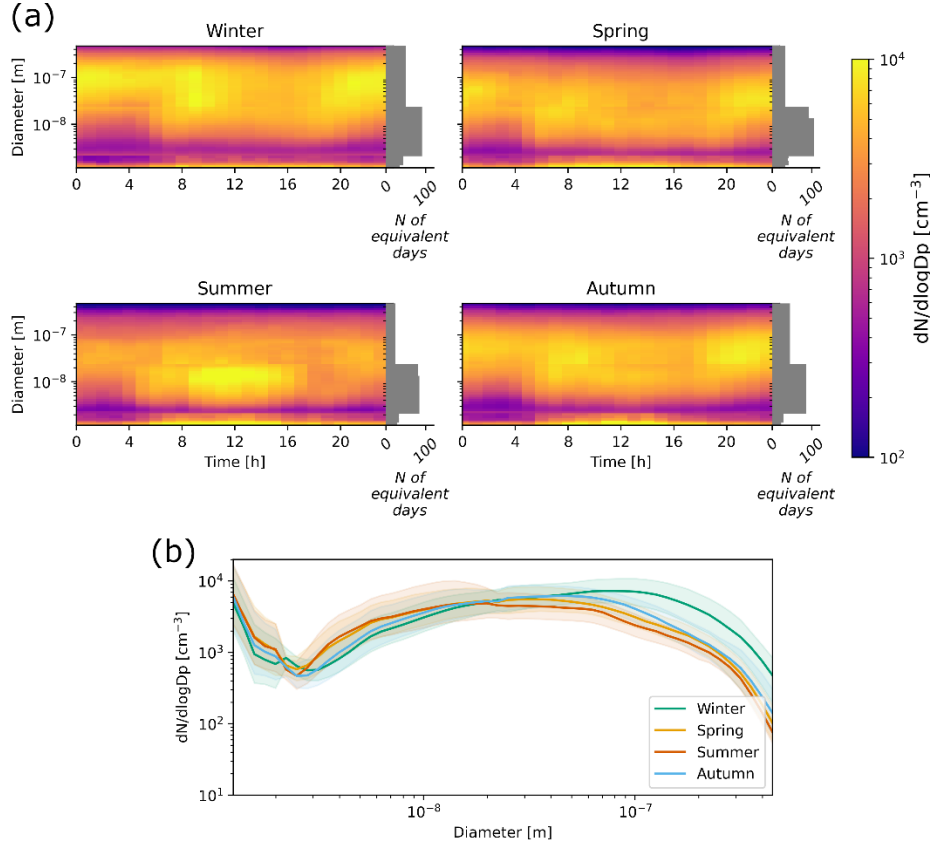


Figure 5: a) Daily median particle number size distribution surface plot per season. The bar plots report the number of equivalent days used to calculate the medians, computed as the total number of 15-minute data points divided by 96 (the number of 15-minute intervals in one day). Times are in Central European Time, UTC+1; b) median particle number size distribution per season. The shaded areas represent the interquartile ranges.

For consistency, the number of data points was also changed to the number of equivalent days in Fig. 6.

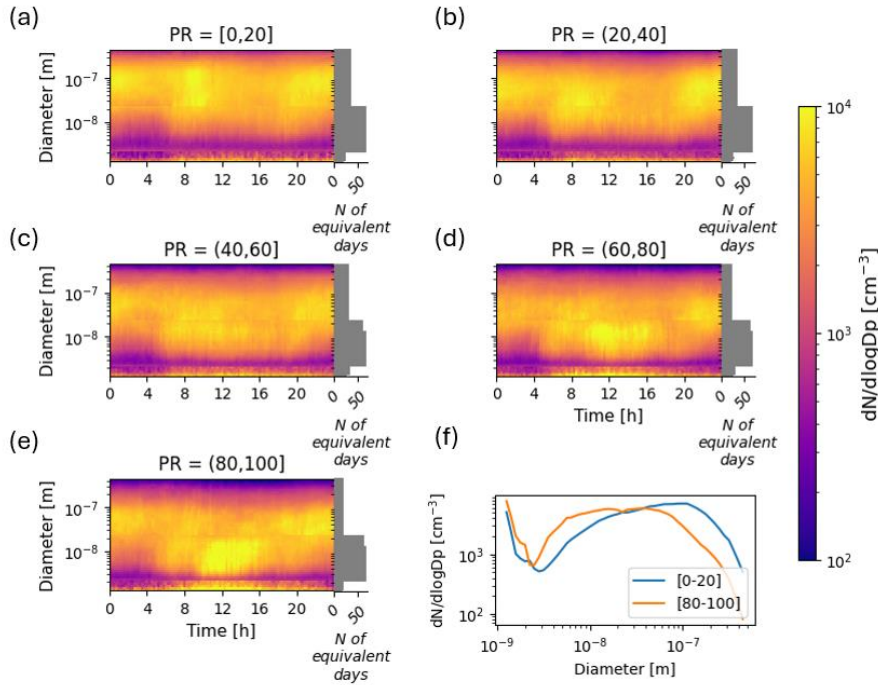


Figure 6: Daily median particle number size distribution surface plots, grouped into 20-percentile intervals of NPF rank (PR; panels a–e). The bar plots indicate the number of equivalent days used to calculate the medians. For the definition of equivalent days, see Fig. 5. Times are in Central European Time (UTC+1). Panel f shows the median size distributions for days with NPF rank below the 20th percentile and above the 80th percentile.

- Lines 315-324: This conclusion that measuring at a smaller cutoff size increases particle number is expected. While there is an important policy discussion to be had regarding the appropriate cutoff diameter, in the absence of further analysis, this section (and the associated figure) does not add to the analysis and could be deleted.

The paragraph was changed to justify the importance of this study and of the measurement of sub-10 nm particles. For details, see the reply to Anonymous Referee #2.

- Figure 7 and lines 348-349: That the sub 2.5 nm particles increase first followed by larger sizes, is not apparent from the figure. I suggest adding an inset or a second panel so that zooms in on the few hours of interest so that the reader can better visualize this trend.

Figure 7 was updated as follows. To identify the point where each curve begins to rise, we computed the derivative of the curve (the difference between consecutive points over time). The first point with the derivative larger than 0.03 was considered to be the beginning of the growth. This threshold was chosen empirically by testing different values.

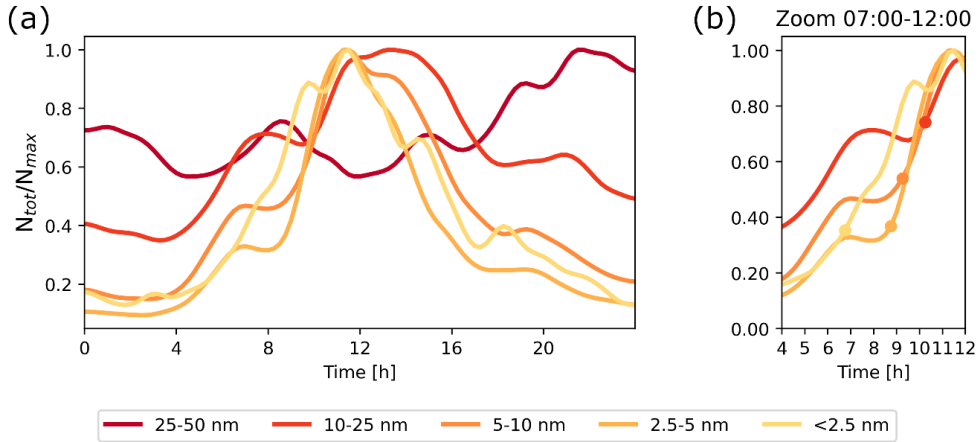


Figure 7: a) The lines represent the median total concentration of particles in different size bins (<2.5 , $2.5-5$, $5-10$, $10-25$, $25-50$ nm), calculated including the days above the 80th percentile of NPF rank. Each line is normalized to its own maximum value and smoothed through a one-dimensional Gaussian filter with a standard deviation of $\sigma = 2$ samples; b) zoom of the time interval between 7 and 12. The dots represent the first point where the derivative of the curve was larger than 0.03 and they mark the beginning of the growth for each curve. The value 0.03 was chosen empirically.

Figure 7: Please include details about the gaussian filter so that the processing steps taken on the data are more transparent.

More details about the Gaussian filter were included in the description of Fig. 7 with the following sentence: “*Each line is normalized to its own maximum value and smoothed through a one-dimensional Gaussian filter with a standard deviation of $\sigma = 2$ samples.*”

- Figure 12: Please include a marker for the study site.

Figure 12 was updated as follows.

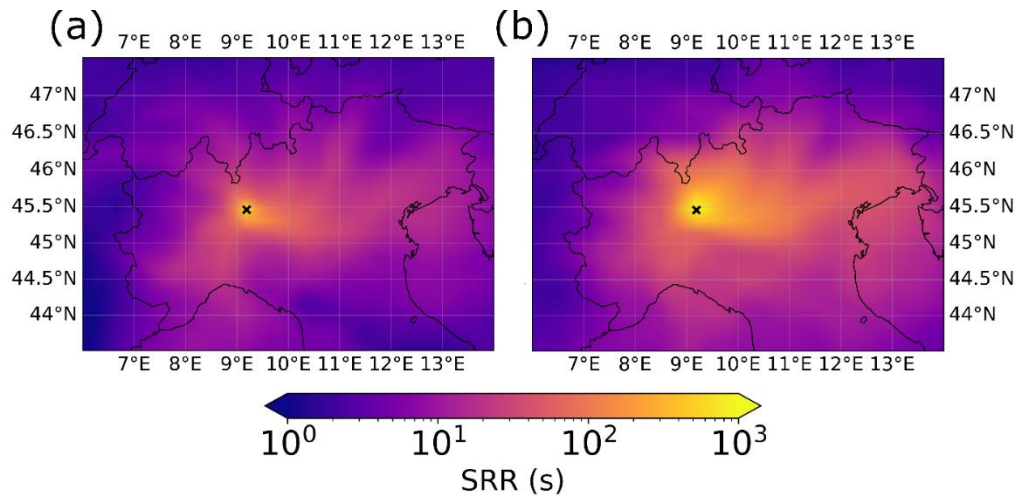


Figure 12: Source-receptor relationship (SRR) below 500 m during a) strong NPF days (percentile rank > 80) and during b) weak NPF days (percentile rank < 20). The x marks indicate the study site.

- Lines 451-452 and Fig. 14: The seasonal change in SO₂ to H₂SO₄ conversion (i.e. due to increased OH) and not just CS could potentially explain these results. This analysis should be considered with greater nuance or should be removed as it does not add much beyond what has been presented previously for CS.

A more detailed analysis was performed to better understand the relation between CS, sulfuric acid, SO₂, and NPF intensity. Section 3.4 was updated as follows.

The role of sulfuric acid, which has been identified in previous studies as a critical precursor vapor in the Po Valley (Cai et al., 2024), was investigated through its proxy, calculated as described in Sect. 2.4.5. The sulfuric acid proxy exhibited an increasing trend with the percentile of NPF rank (Fig. 14a), suggesting its potential contribution to the NPF process.

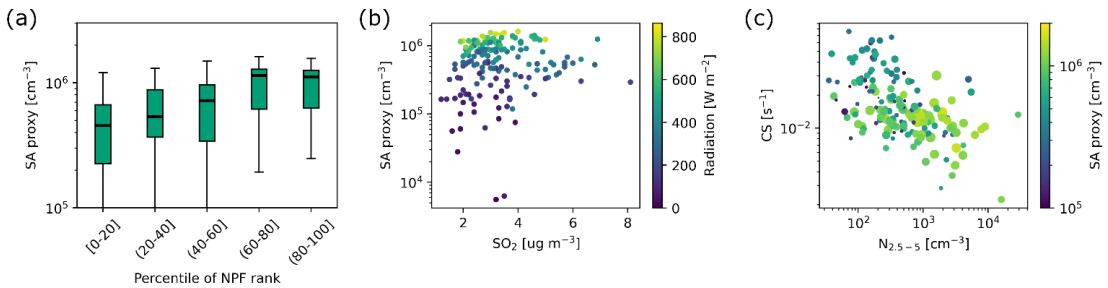


Figure 14: a) Sulfuric acid (SA) proxy daily median calculated over the active time window per rank class. For the description of the boxplots, refer to Fig. 4b; b) relation between sulfuric acid (SA) proxy, SO₂ concentration, and radiation; c) relation between CS, sulfuric acid (SA) proxy, and N_{2.5-5}, representing NPF intensity as explained in Sect. 2.4.1. The size of the dots represents the radiation. For both panels b and c, each point is the daily median calculated over the active time window.

No clear correlation between sulfuric acid and SO₂ concentrations was observed (Fig. 14b), indicating that SO₂ was not a limiting factor for sulfuric acid formation in Milan. On the other hand, sulfuric acid showed a clear increase with radiation (Fig. 14b and more clearly, Fig. S8), hinting at the role of photochemical processes for its formation rather than SO₂ availability or a sink effect. Indeed, while on average, a higher sulfuric acid proxy was recorded in correspondence with lower CS (Fig. S8), several cases with low CS and low sulfuric acid were observed and were linked to low radiation.

The relative roles of CS and sulfuric acid in NPF were then investigated using the concentration of 2.5-5 nm particles as a proxy for NPF intensity (Sect. 2.4.1). Figure 14c clearly presents an inverse correlation between N_{2.5-5} and CS, indicating the relevant role of the CS in enhancing the NPF mechanism. On average, higher concentrations of sulfuric acid proxy were associated with stronger NPF (Fig. 14a and Fig. 14c). However, given the large variability in the trend, its role is less clear. The gaps in the CS time series due to the limited SMPS data coverage are reflected into the SA proxy time series and may affect Fig. 14.

The following figure was added in the Supplementary Materials:

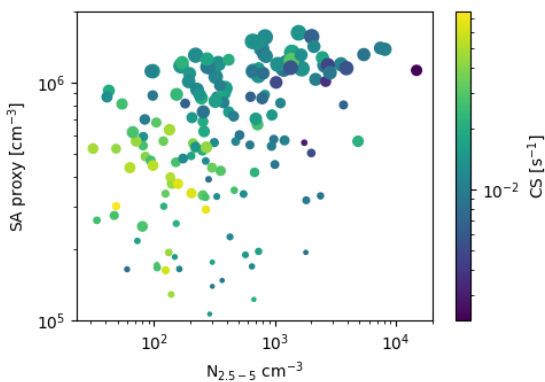


Figure S8: Relation between CS, sulfuric acid (SA) proxy, and $N_{2.5-5}$. The size of the dots represents the radiation. Each point corresponds to the daily median over the active time window.

- I encourage the authors to consider depositing their data in a repository. Given the variability of NPF in urban environments that is discussed in the manuscript, it is clear that measurements in a single location are inadequate to understand the variability and controlling factors of NPF. Accessibility of data from various environments will aid in improving our understanding of NPF.

The data were made available, and the following sentence was added in the article:

“The size distribution data from the nCNC, NAIS, and SMPS presented in this work are publicly available at <https://doi.org/10.5281/zenodo.18130252> (Agrò, 2026).”

References

Agrò, M.: Data of "Ventilation and low pollution enhancing new particle formation in Milan, Italy", Zenodo, <https://doi.org/10.5281/zenodo.18130252>, 2026.

Batchvarova, E. and Gryning, S.-E.: Applied model for the growth of the daytime mixed layer, *Boundary-Layer Meteorol.*, 56, 261–274, <https://doi.org/10.1007/BF00120423>, 1991.

Bettineschi, M., Vitali, B., Cholakian, A., Zardi, D., Bianchi, F., Sinclair, V., Mikkola, J., Cristofanelli, P., Marinoni, A., Mazzini, M., Heikkinen, L., Aurela, M., Paglione, M., Bessagnet, B., Tuccella, P., and Ciarelli, G.: Across land, sea, and mountains: sulphate aerosol sources and transport dynamics over the northern Apennines, *Environ. Sci.: Atmos.*, 5, 1023–1034, <https://doi.org/10.1039/D5EA00035A>, 2025.

Cai, J., Sulo, J., Gu, Y., Holm, S., Cai, R., Thomas, S., Neuberger, A., Mattsson, F., Paglione, M., Decesari, S., Rinaldi, M., Yin, R., Aliaga, D., Huang, W., Li, Y., Gramlich, Y., Ciarelli, G., Quéléver, L., Sarnela, N., Lehtipalo, K., Zannoni, N., Wu, C., Nie, W., Kangasluoma, J., Mohr, C., Kulmala, M., Zha, Q., Stolzenburg, D., and Bianchi, F.: Elucidating the mechanisms of atmospheric new particle formation in the highly

polluted Po Valley, Italy, *Atmospheric Chemistry and Physics*, 24, 2423–2441, <https://doi.org/10.5194/acp-24-2423-2024>, 2024.

Gormley, P. G. and Kennedy, M.: Diffusion from a Stream Flowing through a Cylindrical Tube, *Proceedings of the Royal Irish Academy. Section A: Mathematical and Physical Sciences*, 52, 163–169, 1948.

Kerminen, V.-M., Chen, X., Vakkari, V., Petäjä, T., Kulmala, M., and Bianchi, F.: Atmospheric new particle formation and growth: review of field observations, *Environ. Res. Lett.*, 13, 103003, <https://doi.org/10.1088/1748-9326/aadf3c>, 2018.

Kulmala, M., Petäjä, T., Nieminen, T., Sipilä, M., Manninen, H. E., Lehtipalo, K., Dal Maso, M., Aalto, P. P., Junninen, H., Paasonen, P., Riipinen, I., Lehtinen, K. E. J., Laaksonen, A., and Kerminen, V.-M.: Measurement of the nucleation of atmospheric aerosol particles, *Nat Protoc.*, 7, 1651–1667, <https://doi.org/10.1038/nprot.2012.091>, 2012.

Kulmala, M., Junninen, H., Dada, L., Salma, I., Weidinger, T., Thén, W., Vörösmarty, M., Komsaare, K., Stolzenburg, D., Cai, R., Yan, C., Li, X., Deng, C., Jiang, J., Petäjä, T., Nieminen, T., and Kerminen, V.-M.: Quiet New Particle Formation in the Atmosphere, *Front. Environ. Sci.*, 10, 912385, <https://doi.org/10.3389/fenvs.2022.912385>, 2022.

Lehtipalo, K., Ahonen, L. R., Baalbaki, R., Sulo, J., Chan, T., Laurila, T., Dada, L., Duplissy, J., Miettinen, E., Vanhanen, J., Kangasluoma, J., Kulmala, M., Petäjä, T., and Jokinen, T.: The standard operating procedure for Airmodus Particle Size Magnifier and nano-Condensation Nucleus Counter, *Journal of Aerosol Science*, 159, 105896, <https://doi.org/10.1016/j.jaerosci.2021.105896>, 2022.

Nieminen, T., Lehtinen, K. E. J., and Kulmala, M.: Sub-10 nm particle growth by vapor condensation – effects of vapor molecule size and particle thermal speed, *Atmospheric Chemistry and Physics*, 10, 9773–9779, <https://doi.org/10.5194/acp-10-9773-2010>, 2010.

Trechera, P., Garcia-Marlès, M., Liu, X., Reche, C., Pérez, N., Savadkoohi, M., Beddows, D., Salma, I., Vörösmarty, M., Casans, A., Casquero-Vera, J. A., Hueglin, C., Marchand, N., Chazeau, B., Gille, G., Kalkavouras, P., Mihalopoulos, N., Ondracek, J., Zikova, N., Niemi, J. V., Manninen, H. E., Green, D. C., Tremper, A. H., Norman, M., Vratolis, S., Eleftheriadis, K., Gómez-Moreno, F. J., Alonso-Blanco, E., Gerwig, H., Wiedensohler, A., Weinhold, K., Merkel, M., Bastian, S., Petit, J.-E., Favez, O., Crumeyrolle, S., Ferlay, N., Martins Dos Santos, S., Putaud, J.-P., Timonen, H., Lampilahti, J., Asbach, C., Wolf, C., Kaminski, H., Altug, H., Hoffmann, B., Rich, D. Q., Pandolfi, M., Harrison, R. M., Hopke, P. K., Petäjä, T., Alastuey, A., and Querol, X.: Phenomenology of ultrafine particle concentrations and size distribution across urban Europe, *Environment International*, 172, 107744, <https://doi.org/10.1016/j.envint.2023.107744>, 2023.

Wagner, R., Manninen, H. E., Franchin, A., Lehtipalo, K., Mirme, S., Steiner, G., Petäjä, T., and Kulmala, M.: On the accuracy of ion measurements using a Neutral cluster and Air Ion Spectrometer, 2016.

Wang, S. C. and and Flagan, R. C.: Scanning Electrical Mobility Spectrometer, *Aerosol Science and Technology*, 13, 230–240, <https://doi.org/10.1080/02786829008959441>, 1990.

Zilitinkevich, S. and Baklanov, A.: Calculation Of The Height Of The Stable Boundary Layer In Practical Applications, *Boundary-Layer Meteorology*, 105, 389–409, <https://doi.org/10.1023/A:1020376832738>, 2002.

Zilitinkevich, S., Esau, I., and Baklanov, A.: Further comments on the equilibrium height of neutral and stable planetary boundary layers, *Quarterly Journal of the Royal Meteorological Society*, 133, 265–271, <https://doi.org/10.1002/qj.27>, 2007.